Earth, Moon, and Planets (2018) 122:1–13
https://doi.org/10.1007/s11038-018-9518-0

The Temperature Regime of the Proposed Landing Sites for the Luna-Glob Mission in the South Polar Region of the Moon

E. A. Feoktistova[1] · **S. G. Pugacheva**[1] · **V. V. Shevchenko**[1]

Received: 7 November 2017 / Accepted: 6 August 2018 / Published online: 10 August 2018

Abstract
In this paper, we investigated the possibility of existence of the hydrogen-containing volatile compounds, similar to those found in the Cabeus crater, in the area of the proposed landing ellipses of the Luna-Glob mission. We found that the existence of water ice and other hydrogen-containing substances is possible only in the presence of a shielding layer of regolith. The time of existence of such deposits does not exceed several tens or hundreds years for a layer of regolith with a thickness of 0.4 m and several thousand years for a layer of regolith 1 m thick.

Keywords Moon · Polar region · Landing sites

1 Introduction

Currently, three areas located in the south polar region of the Moon are selected as the possible landing sites of the Luna-Globe mission. According to the requirements to be met by the proposed landing sites, these areas are ellipses with a size of 15×30 km, the semi-major axis of which is elongated in the meridian direction, located in the sector (65÷85°S and 0÷60°E) (Flahaut et al. 2016). In the list of proposed landing sites for the Luna-Globe mission (Flahaut et al. 2016), these areas have been specified as the landing ellipses 1, 4 and 6. The landing ellipse 1 with its center at the point (68.8°S, 21.2°E) is located to the south-west of the Manzinus crater (67.3°S, 26.2°E) (Fig. 1a), the landing ellipse 4 (coordinates of the center of the ellipse: 68.6°S, 11.6°E) is located further north-west than the Simpelius crater (69.9°S, 16.1°E) (Fig. 1b), and the landing ellipse 6 with the center at the point (69.5°S, 43,5°E) is located to the south of the Boussingault crater(70.1°S, 53.4°E) (Fig. 1c).

✉ E. A. Feoktistova
Hrulis@yandex.ru

[1] Sternberg State Astronomical Institute, M.V. Lomonosov Moscow State University, Universitetskyprospekt 13, Moscow, Russian Federation 119992

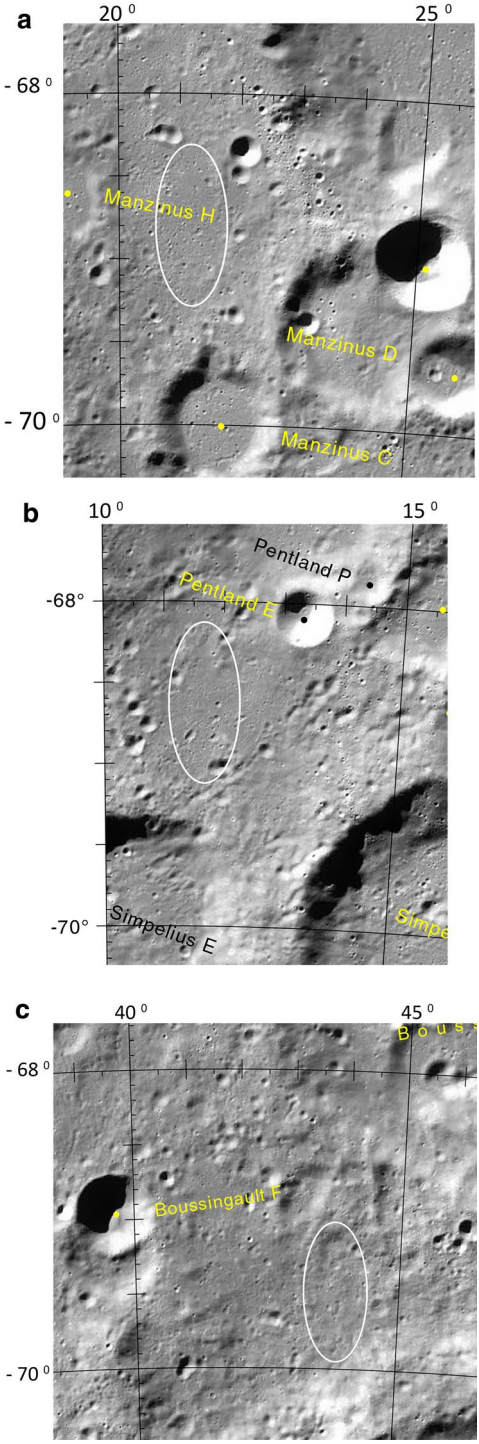

Fig. 1 Areas in which the landing ellipses are located: of **a** ellipse 1, **b** ellipse 4, and **c** ellipse 6. The boundaries of the landing ellipses are shown by the white line. Fragment of the 1:1 Million-Scale Maps of the Moon

2 Calculation of Insolation and Temperatures

The heat balance of an element of the lunar surface is determined by the ratio of the flux of direct solar radiation incident on the given surface element, the fluxes of reflected and infrared radiation from all adjacent illuminated surface elements visible from a given element, and the heat flux from the Moon's interior. The values of all these summands (excluding the value of the flux from the Moon's interior, 0.016 W/m^2) are determined by the surface geometry and the thermophysical properties of the soil of the investigated site (Langseth et al. 1976). For our studies, we have used data provided by (Karachevtseva et al. 2015) containing information on the surface elements in latitude and longitude increments of 0.01° in the format of latitude, longitude, slope (α), orientation (β) and altitude of the surface element. According to these data, the altitude difference in the area of ellipse 1 is 0.3 km: from 0.6 to 0.9 km, the minimum values of altitudes are observed in the northern part of the ellipse, and the maximum ones—in the southern part. The altitude difference in the area of ellipse 4 is smaller and is 0.2 km: from 0.7 to 0.9 km, with maximum altitudes observed in the southern part of the ellipse, and minimum ones—in the northern part. In the area of the ellipse 6, the altitude difference is 0.3 km: from 0.4 in the northern and central parts to 0.7 km in the southern part. These geomorphological parameters have been used to calculate the insolation and temperature conditions of the investigated regions. The position of the Sun for each moment of time has been determined by its coordinates in the horizontal system: zenith distance and azimuth. The time increment corresponds to the Sun's azimuth displacement by 1°. Figure 1 shows the results of insolation calculations in the investigated areas. We used a time period equal to one lunar year in our calculations.

The calculation of the thermal conditions of the lunar surface in the area of the landing ellipses 1, 4 and 6 has been carried out using a two-layer soil model similarly to that described in the studies (Vasavada et al. 1999; Wohler et al. 2017). According to this model, the surface layer of the lunar soil can be represented as consisting of 2 layers: the upper dust layer has a thickness of 2–3 cm and is characterized by low density (1000–1300 kg/m^3 (Vasavada et al. 1999)) and low thermal conductivity. The thickness of the second layer is estimated as 3–5 m, with an average density of 1800 g/m^3 (Vasavada et al. 1999) and higher thermal conductivity. These layers form regolith—a fragmented material formed as a result of repeated crushing and mixing of rocks by meteorite bombardment, as well as under the influence of solar and galactic radiation.

To obtain the temperature distribution with depth was obtained by the solution of nonlinear heat-diffusion equation by method of finite differences (Samarsky 1977).To solve this equation, we have taken into account the direct solar flux incident on each illuminated element of the surface, flux reflected from the other illuminated elements, flux of infrared radiation emitted from other elements and the internal thermal flux. We don't take into account the thermal flux from the adjacent elements of the crater; however, this flux can be ignored because of the low thermal conductivity of regolith on the Moon. The heat at the initial step of calculations the temperature along the whole depth was set to 100 K. To reduce the influence of the initial set of the temperature distribution, the calculations were performed for 100 lunar years. Since the upper boundary condition is nonlinear relatively temperature, the temperature at the surface at each time step was calculated by the method of simple iteration.

3 Results of Calculation

Figure 2 shows the illumination conditions of the landing ellipses 1, 4 and 6 (the boundaries of the landing ellipses are shown by the black line). For the point located at the center of the landing ellipse 1, the maximum altitude of the Sun during the year varies from 19.7° above the horizon to 22.7° above the horizon. The surrounding relief does not significantly affect the illumination in this point: the maximum altitude of the horizon does not exceed 2.6°, thus, this point is shaded by the surrounding relief within 1.5% of the duration of a lunar year. Figure 2a shows that the illumination in the area of the landing ellipse 1 does not exceed 45% for a period equal to one lunar year.

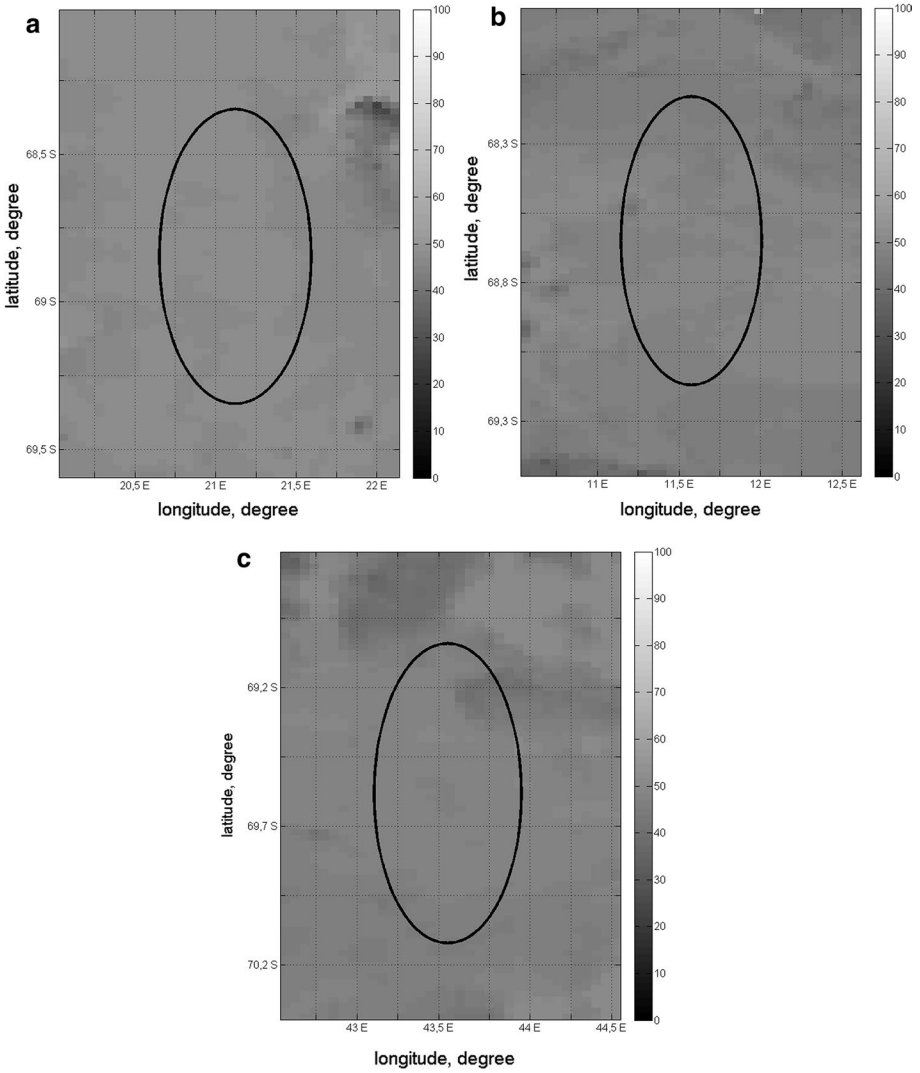

Fig. 2 The illumination (in percent) of **a** ellipse 1, **b** ellipse 4, and **c** ellipse 6

For the point located at the center of the landing ellipse 4, the maximum altitude of the Sun varies from 19.9° to 22.9° above the horizon during the year. According to our calculations, the altitude of the horizon does not exceed 2.2° in the northeastern direction and 2.6° in the northwestern one. Due to this, the surrounding relief affects illumination in the center of the landing ellipse 4 only within 1.6% of a lunar year. The distribution of illumination in the area of the landing ellipse 4 is shown in Fig. 2b. This value varies from 50% in the central part of the ellipse to 40–45% in its northern and southern parts.

The maximum altitude of the Sun at the point located in the center of the landing ellipse 6 varies from 18.9° to 22° (Fig. 2c). The height of the surrounding relief is up to 3.6° with maximum in the northeast direction from the center of the landing ellipse. As can be seen from Fig. 2c, the illumination in the area of the landing ellipse 6 varies from 45% in its southern part to 50% in the central one. The greatest illumination is observed in its northern part, where, due to the unevenness of the relief, it reaches 60% for a period equal to a lunar year.

The obtained distribution of maximum and minimum (night) temperatures in the area of the landing ellipses is shown in Figs. 3 and 4. Maximum temperatures in the areas of ellipses 1 and 4 do not exceed 300–330 K (Fig. 3a, b). In the area of the ellipse 6, the maximum temperatures lie in the range from 290 K in the northern part of the ellipse to 240–310 K in its southern part (Fig. 3c). Minimum temperatures in the area of the landing ellipses 1 and 4 do not exceed 85 K (Fig. 4a, b) falling to 80 K in the northwestern part of the ellipse 4.

The distribution of minimum temperatures in the area of the ellipse 6 is less uniform: here, the spread in values is from 76 to 80 K in the central and northern parts to 85 K in the southern one (Fig. 4c).

The neutron spectrometer of the Lunar Prospector (LP) probe has detected a decrease in the epithermal neutron flux in the area of these ellipses, which has been interpreted as the presence of increased hydrogen content in the soil of these areas: 61.9 ppm, 56.7 ppm and 77.9 ppm in the ellipses 1, 4 and 6, respectively (Flahaut et al. 2016), with an average hydrogen content in the Moon's soil of 50–55 ppm (Feldman et al. 2001). These results have been confirmed by the data from the Lunar Exploration Neutron Detector (LEND) of the Lunar Reconnaissance Orbiter (LRO) probe, which had also discovered an increased hydrogen content in these areas (Flahaut et al. 2016). Thus, according to the data obtained by the neutron spectrometer LP, hydrogen content in the area of the landing ellipse 4 is close to the mean value, and higher in the areas of the ellipses 1 and 6.

There are several sources of hydrogen-containing compounds in the polar regions of the Moon: (1) solar wind, protons of which, interacting with regolith of the Moon, can be implanted into regolith particles or can form molecules of water, some of which migrating may subsequently accumulate in "cold traps" near the poles (Crider and Vondrak 2000; Starukhina 2001); (2) collisions of asteroids, comets or micrometeorites with the surface of the Moon, at which chemical compounds such as H_2O, CO, CO_2, S, SO_2, H_2 are released; (3) degassing of the Moon's interior, which leads to the release of such compounds as CO, COS, CS, CS_2, SO and CO_2, and that was active at an early stage of the evolution of the Moon (Fegley 1991) and apparently has lost its importance till now.

The depositions of these compounds in the permanently shaded area in the Cabeus crater have been detected during an impact test of the Lunar Crater Observation and Sensing Satellite probe (LCROSS) (Gladstone et al. 2010; Colaprete et al. 2010). The content of water in the release has reached $1.5 \pm 4\%$ according to data (Mitrofanov et al. 2010) or according to estimates (Colaprete et al. 2010): $5.6 \pm 2.9\%$.

The lifetime of such deposits is determined by the rate of their vaporization, which is a function of temperature. In a number of studies (Zhang and Paige 2009), the temperatures

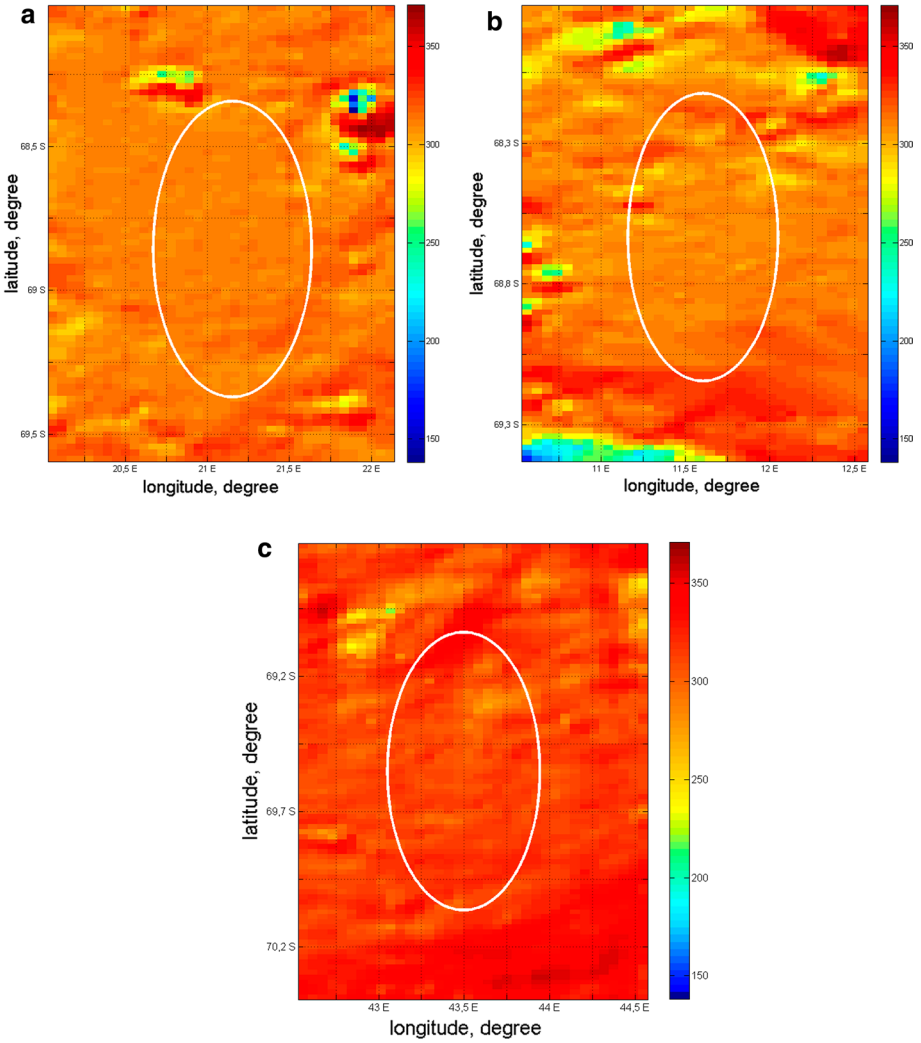

Fig. 3 Diurnal maximum temperatures in the areas of **a** ellipse 1, **b** ellipse 4, and **c** ellipse 6

at which the deposits of volatile compounds can be stable with respect to vaporization have been calculated (the temperature at which deposits of 1 mm thickness vaporize over 1 billion years has been assumed as a criterion of stability). For water ice, this value is 106.6 K (Paige et al. 2010), for CO_2, NH_3, SO_2, H_2S—54.3, 65.5, 62.3 the value is 50.6 K, respectively (Paige et al. 2010), and for compounds such as C_2H_4, and CH_3OH: 41.4 the value is 92 K, respectively. As the calculation results show, in the area of the landing ellipses 1, 4 and 6, the maximum temperatures are too high, and the deposits of volatile compounds similar to those found in the area of the Cabeus crater, including water ice, cannot exist on the surface. As is known, the rate of vaporization of volatile compounds is significantly reduced when there is a shielding layer of regolith (Vasavada et al. 1999). The neutron spectrometer of the LP probe has received data on hydrogen content in the upper soil layer with a depth of up to 0.4–0.5 m. Information obtained by the LEND neutron spectrometer refers to the soil layer

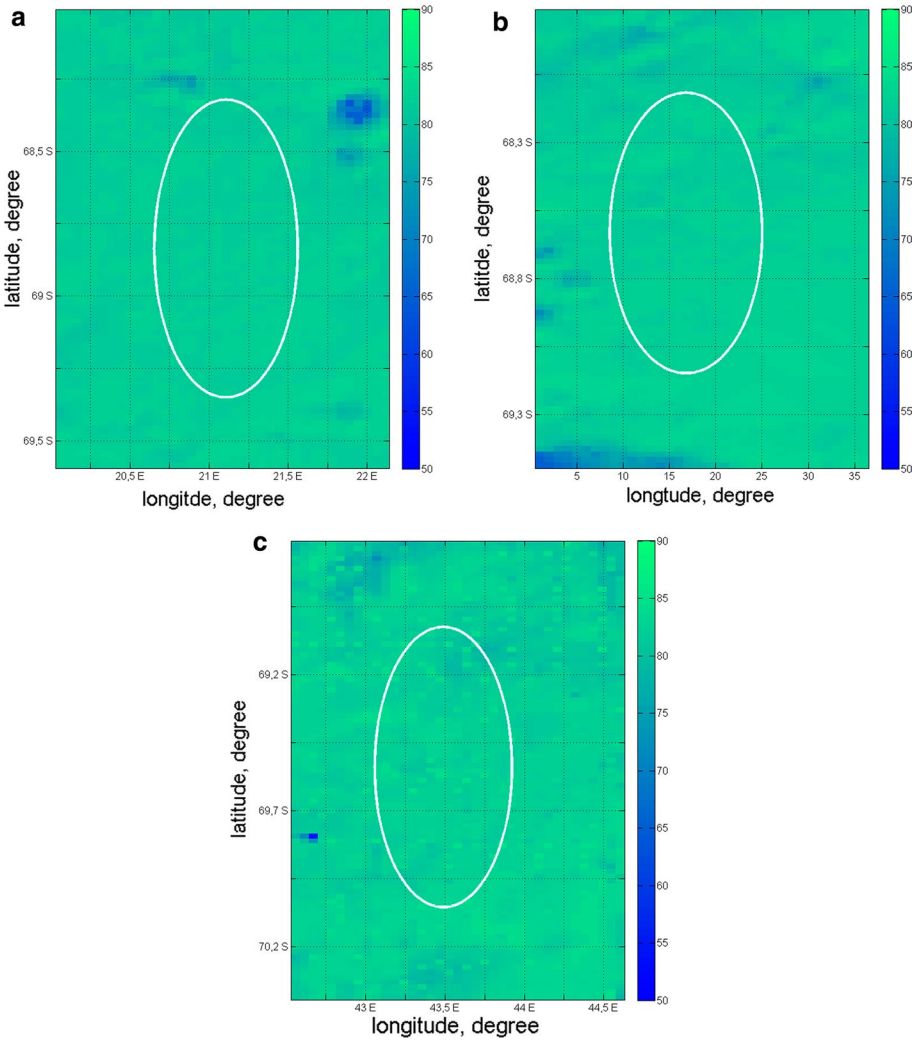

Fig. 4 Diurnal minimal temperatures in the areas of **a** ellipse 1, **b** ellipse 4, and **c** ellipse 6

with a thickness of 1–1.5 m. Thus, it can be assumed that the deposits of water ice, if they exist in these areas, can be under a layer of regolith with a thickness from 0.4 to 1.5 m. The rate of sublimation of ice screened by a layer of silicate material is determined by the magnitude of the flow of water molecules at the ice-regolith boundary. The value of the flow is expressed by the formula (Schorghofer and Taylor 2007):

$$J = \mu l E / 2\Delta z$$

where μ—mass of the water molecules ($2.99 * 10^{-26}$ kg); l—the size of the soil granules (75 μm) (Schorghofer and Taylor 2007), Δz—thickness of the regolith layer (calculations were made for values: 0.4 m and 1 m); E—the rate of evaporation of ice, determined according to Watson (1961) as:

$$E = aP/\left[2\pi kT\mu\right]^{1/2}$$

where a is the condensation coefficient assumed here as 1, k is the Boltzmann constant, P is the saturated vapor pressure, and T is the temperature at the ice-regolith boundary. Regolith has been modeled as consisting of two layers, similar to how it has been in calculating the temperature conditions. As a result, it has been found that the existence of water ice deposits in the area of all three landing ellipses is possible with the presence of a screening layer of regolith (Figs. 5 and 6). At the same time, for the layer with a thickness of 0.4 m, the lifetime of such deposits does not exceed 2 years, in the central part of the landing ellipse 1 year and 10 thousand years in its north part (Fig. 5a). In the central part of the ellipse 4, the lifetime of the water ice deposits with a shielding regolith layer reaches 50 years, and in the northeastern region—up to 5000 years (Fig. 5b). Along existence of water ice deposits is possible in the area of the land in ellipse 6 (Fig. 5c). In the central and northern parts of the ellipse, the lifetime of such deposits in certain small areas reaches hundreds and thousands of years.

The lifetime of water ice deposits increases significantly if the thickness of the regolith layer reaches 1 m. Nevertheless, in the central part of the ellipses 1 and 4, the lifetime of water ice, according to our calculations, does not exceed 100–130 years, even with a screening layer of regolith with a thickness of 1 m (Fig. 6a, b). In the northern part of the ellipse 1 there are separate regions where the lifetime of the deposits of water ice reaches 1 billion years and they can be considered stable against evaporation. The longer lifetime of water ice deposits (> 300 years in its central part and > 75,000 in its northeastern part) is possible in the ellipse 6 (Fig. 6c).

We assume that this is due to terrain unevenness, forming the so-called micro cold trap (McGovernetal et al. 2013), the temperatures in which can be significantly lower than the ambient temperature.

4 Solar Wind as Possible Source of Hydrogen in the Proposed Landing Sites

In addition to the fallout of comets and asteroids, as well as meteorites, the possible source of hydrogen on the surface of the Moon is the solar wind. Let us estimate the amount of hydrogen implanted during the interaction of the solar wind with regolith in the area of the landing ellipses. The hydrogen content in the soil [H] is determined by the ratio (Starukhina 2001):

$$[H] = Sm_p n_s,$$

where S is the specific surface area of the regolith particles, the values of which lie in the range 800–5000 cm^{-2} g^{-1} (Starukhina 2001), m_p is the proton mass, n_s is the number of implanted hydrogen atoms on a unit of surface. $(1.5 \pm 6) \times 10^{16}$ cm^{-2} (Starukhina 2001). Using the values of [H] for the areas of the landing ellipses obtained by the neutron spectrometer of the Lunar Prospector probe, we determine the concentration of hydrogen atoms in these areas (Table 1). As can be seen from the Table, the obtained hydrogen atom concentrations in the areas of the landing ellipses are comparable with the hydrogen concentration in the lunar samples $(1.5 \pm 6) \times 10^{16}$ cm^{-2} (Starukhina 2001). Let us estimate the time required to achieve the observed hydrogen concentrations in the areas of the landing

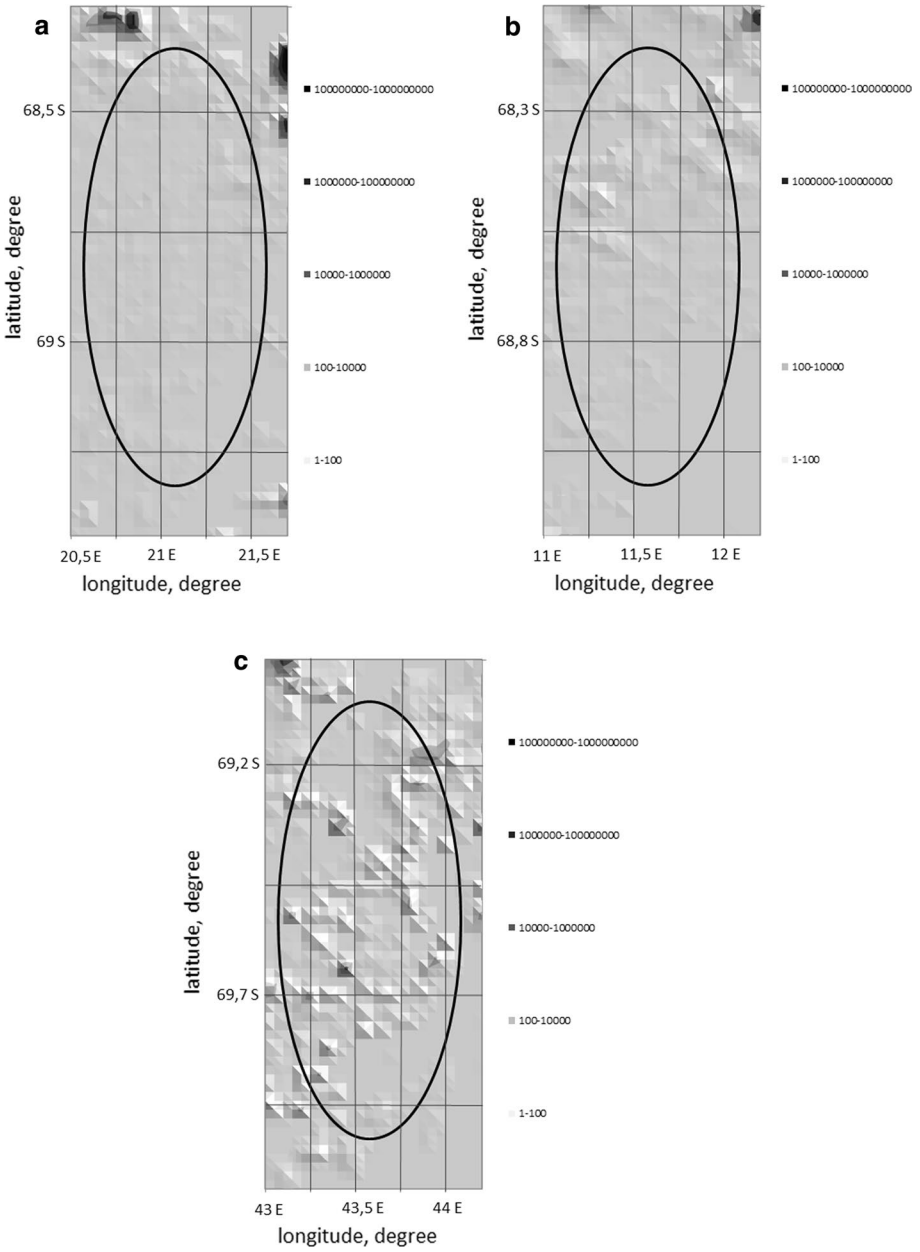

Fig. 5 The lifetime (in years) of water ice deposits under a layer of regolith with a thickness of 0.4 m in the area **a** ellipse 1, **b** ellipse 4, and **c** ellipse 6

ellipses. The time τ_s required to achieve the observed amount of hydrogen depends on the rate of arrival of hydrogen atoms and on the rate of their losses. To calculate the fraction of implanted hydrogen, we take into account the influence of surface topography, as well as

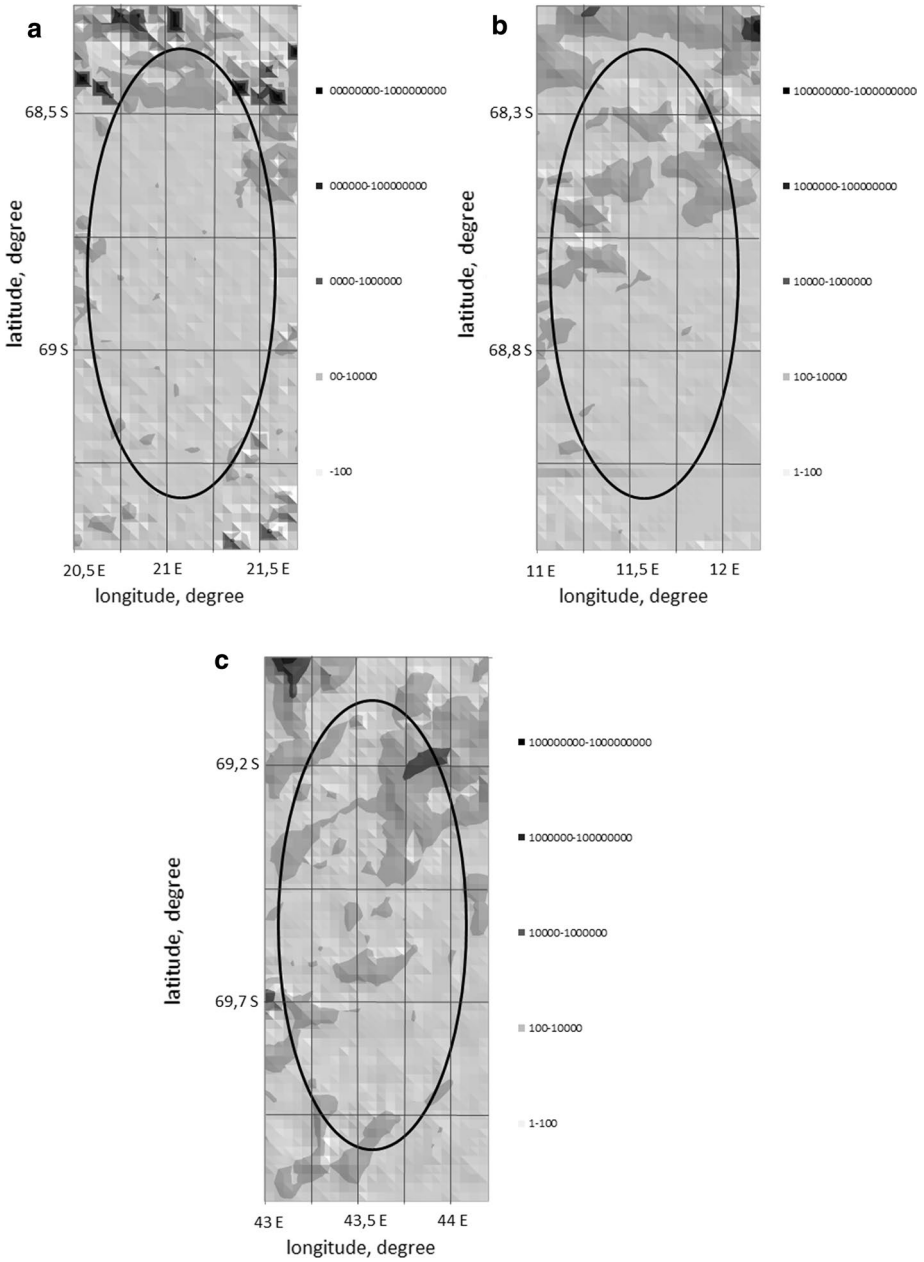

Fig. 6 The lifetime (in years) of water ice deposits under a layer of regolith with a thickness of 1 m in the area **a** ellipse 1, **b** ellipse 4, and **c** ellipse 6″

changes in the altitude of the Sun h_0 by the magnitude of the proton flux of the solar wind falling on a given surface element: where j_0 is the proton flux of the solar wind incident on the Moon's surface,

Table 1 The hydrogen concentrations and the rate of its accumulation which are necessary to achieve the observed hydrogen content at the area of the landing ellipses

	[H] (ppm), (lunar prospector)	n_s (sm^{-2})		τ_s (of years)
		S = 800	S = 5000	
Ellipse 1	61.9	4.6×10^{16}	7.4×10^{15}	250 ÷ 40
Ellipse 4	56.7	4.2×10^{16}	6.8×10^{15}	215 ÷ 30
Ellipse 6	77.9	5.8×10^{16}	9.3×10^{15}	300 ÷ 50

$$j = j_0 * (\sin h_0 * \cos\alpha - \cosh_0 * \sin\alpha * \cos\Delta),$$

where j_0 is the proton flux of the solar wind incident on the Moon's surface, Δ is the angle between the direction to the Sun and the orientation of the surface. The magnitude of the solar wind flux at a distance of the Earth is $4\times10^{-8}/cm^2$ s, but as ~20% of protons are reflected from the Moon's surface without interaction(Wieser et al. 2009), the value $j_0 = 3.2\times10^{-8}/cm^2$ s. As in the calculation of the temperature conditions, the position of the Sun is determined by its azimuth and angular altitude above the horizon. The calculation will be carried out with a time increment equal to the Sun's azimuth displacement by 1°. The decrease in the concentration of hydrogen is due to the influence of such factors as diffusion and sputtering of implanted atoms under the action of the solar wind.

Since diffusion depends on temperature, it does not have a significant effect on the hydrogen concentration in the polar regions, but becomes significant at lower latitudes. The diffusion rate of hydrogen atoms is determined by the formula:

$$D = D_0 \exp(-U/kT),$$

where U is the activation energy, [0.3 ± 3 eV (Starukhina 2001)], T is the surface temperature calculated above. Using the estimates for D_0 from the study (Farrell et al. 2015), according to which the value of D_0 lies in the range $10^{-6} \pm 10^{-14}$ cm^2/s, we estimate the effect of diffusion on the achievement of observed hydrogen concentrations in the area of the landing ellipses. Taking the depth of implantation of hydrogen atoms $h \sim 10^{-6}$ cm, we obtain that the diffusion time for the areas of the landing ellipses varies during the lunar day from 10^{-2} s at noon to 10^{10} s at night.

Table 1 shows the calculated hydrogen concentrations and the rate of its accumulation, which are necessary to achieve the observed values of [*H*] from the data of the neutron spectrometer of the Lunar Prospector probe. As can be seen, small-time periods (~tens and hundreds of years) are sufficient to achieve the observed hydrogen content at the area of the landing ellipses.

These conclusions coincide with the results obtained in (Starukhina 2001). At the same time, these results show that when the solar wind is continuously exposed to these regions for a billion years, the hydrogen concentration in them should be much higher. The observed values of the hydrogen concentration indicate that there are mechanisms of hydrogen loss. In a number of works (Starukhina 2001; Crider and Vondrak 2003) processes were considered that lead to a change in the concentration of implanted hydrogen. Starukhina (2001) proposed that difference in diffusion coefficients can explain different concentrations of hydrogen in lunar regions. Effect of continual processes, such as diffusion, sublimation of water ice and Layman α radiation, and discrete event, such as impact gardening, to hydrogen content in lunar regolith

was investigated in Crider and Vondrak (2003). Crider and Vondrak (2003) demonstrated that effect of these processes at increasing the amount of time does not lead to increased hydrogen concentration.

5 Conclusions

In this study, we have investigated the temperature and illumination (insolation) conditions for the areas of proposed landing sites for the planned mission Luna-Globe. It was shown that the influence of the surrounding relief on insolation in these areas is weak and the areas of the landing ellipses are illuminated during 50–55% of the lunar day. The temperatures of the Moon's surface in the areas of the landing ellipses vary from 300–340 K at day to 80–90 K at night. The data obtained by the neutron spectrometers of the Lunar Prospector probe and LRO probe have shown the presence of an increased hydrogen content in these areas, which may be due to various factors, in particular due the presence of deposits of volatile compounds (water ice) or the accumulation of hydrogen in the surface layer of regolith as a result of influence of protons of the solar wind. We have analyzed the possibility of the existence of water ice deposits in these areas. It has been shown that the lifetime of such deposits in the areas of the landing ellipses is not more than hundreds of millions of years even with the presence of a screening layer of regolith with a thickness of 0.4–1 m. The possibility of hydrogen accumulation under the influence of protons of the solar wind has been investigated too. As a result, it was found that the period of time required to accumulate the observed hydrogen concentrations in the area of the landing ellipses is from several to several hundreds of years. Thus, the increased hydrogen content in these areas can be due to the influence of the solar wind.

References

A. Colaprete, P. Schultz, J. Heldmann, D. Wooden, M. Shirley, K. Ennico, B. Hermalyn, W. Marshall, A. Ricco, R.C. Elphic, D. Goldstein, D. Summy, G.D. Bart, E. Asphaug, D. Korycansky, D. Landis, L. Sollitt, Science **330**, 463–468 (2010)

D.H. Crider, R.R. Vondrak, J. Geophys. Res. **105**, 26773–26782 (2000)

D.H. Crider, R.R. Vondrak, J. Geophys. Res. **108**, 5079 (2003). https://doi.org/10.1029/2002je002030

B. Fegley Jr., GRL **18**, 2073–2076 (1991)

W.C. Feldman, S. Maurice, A.B. Binder, B.L. Barraclough, R.C. Elphic, D.J. Lawrence, J. Geophys. Res. **106**, 23231–23252 (2001)

J. Flahaut, C. Wöhler, A.A. Berezhnoy, D. Rommel, A. Grumpe, E.A. Feoktistova, V.V. Shevchenko, C. Quantin, P. Williams, in *Book of Proceedings 7th Lunar Exploration Symposium*, (2016), pp. 235–245

G.R. Gladstone, D.M. Hurley, K.D. Retherford, P.D. Feldman, W.R. Pryor, J.-Y. Chaufray, M. Versteeg, T.K. Greathouse, A.J. Steffl, H. Throop, J.W. Parker, D.E. Kaufmann, A.F. Egan, M.W. Davis, D.C. Slater, J. Mukherjee, P.F. Miles, A.R. Hendrix, A. Colaprete, S.A. Stren, Science **333**, 1703 (2010)

P. Karachevtseva, A.A. Kokhanov, A.A. Konopikhin, I.E. Nadezhdina, A.E. Zubarev, V.D. Patratiy, N.A. Kozlova, D.V. Uchaev, D.V. Uchaev, V.A. Malinnikov, J. Oberst, Sol. Syst. Res. **49**, 92–109 (2015)

M.G. Langseth, S.J. Keihm, K. Peters, in *Proceedings of the 7th Lunar Science Conference*, vol. 3 (Pergamon Press, New York, 1976), pp. 3143–3171

J.A. McGovern, D.B. Bussey, B.T. Greenhagen, D.A. Paige, J.T.S. Cahill, P.D. Spudis, Icarus **223**(1), 566–581 (2013)

I.G. Mitrofanov, A.B. Sanin, W.V. Boynton, G. Chin, J.B. Garvin, D. Golovin, L.G. Evans, K. Harshman, A.S. Kozyrev, M.L. Litvak, A. Malakhov, E. Mazarico, T. McClanahan, G. Milikh, M. Mokrousov, G. Nandikotkur, G.A. Neumann, I. Nuzhdin, R. Sagdeev, V.V. Shevchenko, V. Shvetsov, D.E. Smith, R.

Starr, V.I. Tretyakov, J. Trombka, D. Usikov, A. Varenikov, A. Vostrukhin, M.T. Zuber, Science **330**, 483–486 (2010)
D.A. Paige, M.A. Siegler, J.A. Zhang, P.O. Hayne, E.J. Foote, K.A. Bennett, A.R. Vasavada, B.T. Greenhagen, J.T. Schofield, D.J. McCleese, M.C. Foote, E. De Jong, B.G. Bills, W. Hartford, B.C. Murray, C.C. Allen, K. Snook, L.A. Soderblom, S. Calcutt, F.W. Taylor, N.E. Bowles, J.L. Bandfield, R. Elphic, R. Ghent, T.D. Glotch, M.B. Wyatt, P.G. Lucey, Science **330**, 479 (2010)
A.A. Samarsky, *Theory of Finite-Difference Schemes* (Nauka, Moscow, 1977)
N. Schorghofer, G.J. Taylor, J. Geophys. Res. **112**, E02010 (2007)
L. Starukhina, J. Geophys. Res. **106**, E7 (2001)
A.R. Vasavada, D.A. Paige, S.E. Wood, Icarus **141**, 179–193 (1999)
K. Watson, B.C. Murray, H. Brown, J. Geophys. Res. **66**, 3033–3045 (1961)
M. Wieser, S. Barabash, Y. Futaana, M. Holmström, A. Bhardwaj, R. Sridharan, M.B. Dhanya, P. Wurz, A. Schaufelberger, K. Asamura, Planet. Space Sci. **57**, 2132–2134 (2009). https://doi.org/10.1016/j.pss.2009.09.012
C. Wohler, A. Grumpe, A.A. Berezhnoy, E.A. Feoktistova, N.A. Evdokimova, K. Kapoor, V.V. Shevchenko, Icarus **285**, 118–136 (2017)
J.A. Zhang, D.A. Paige, Geophys. Res. Lett. **37**, L16203 (2009)